Cell Calcium 78 (2019) 66–75

Contents lists available at ScienceDirect

Cell Calcium

journal homepage: www.elsevier.com/locate/ceca

Methylglyoxal evokes acute Ca^{2+} transients in distinct cell types and increases agonist-evoked Ca^{2+} entry in endothelial cells via CRAC channels

Robin Sachdeva[a], Thomas Fleming[b,c], Dagmar Schumacher[a], Sarah Homberg[a], Kathrin Stilz[a], Franziska Mohr[d], Andreas H. Wagner[d], Volodymyr Tsvilovskyy[a], Ilka Mathar[a], Marc Freichel[a,*]

[a] Institute of Pharmacology, Heidelberg University, Im Neuenheimer Feld 366, 69120 Heidelberg, Germany
[b] Department of Medicine I and Clinical Chemistry, Heidelberg University Hospital, Germany
[c] German Center for Diabetes Research (DZD), Germany
[d] Institute of Physiology and Pathophysiology, Division of Cardiovascular Physiology, Im Neuenheimer Feld 326, 69120 Heidelberg, Germany

ARTICLE INFO

Keywords:
Methylglyoxal
Endothelial cells
Calcium entry
Calcium release activated calcium (CRAC) channels

ABSTRACT

Methylglyoxal (MG) is a by-product of glucose metabolism and its accumulation has been linked to the development of diabetic complications such as retinopathy and nephropathy by affecting multiple signalling pathways. However, its influence on the intracellular Ca^{2+} homeostasis and particularly Ca^{2+} entry, which has been reported to be mediated via TRPA1 channels in DRG neurons, has not been studied in much detail in other cell types. In this study, we report the consequences of acute and long-term MG application on intracellular Ca^{2+} levels in endothelial cells. We showed that acute MG application doesn't evoke any instantaneous changes in the intracellular Ca^{2+} concentration in immortalized mouse cardiac endothelial cells (MCECs) and murine microvascular endothelial cells (muMECs). In contrast, an MG-induced rise in intracellular Ca^{2+} level was observed in primary mouse mesangial cells within 30 s, indicating that the modulation of Ca^{2+} homeostasis by MG is strictly cell type specific. The formation of the MG-derived advanced glycation end product (AGE) MG-H1 was found to be time and concentration-dependent in MCECs. Likewise, MG pre-incubation for 6 h increased the angiotensin II-evoked Ca^{2+} entry in MCECs and muMECs which was abrogated by inhibition of Calcium release activated calcium (CRAC) channels with GSK-7975A, but unaffected by an inhibitor specific to TRPA1 channels. Quantitative PCR analysis revealed that MG pre-treatment did not affect expression of the genes encoding the angiotensin receptors AT1R (Agtr 1a & Agtr 1b), Trpa1 nor Orai1, Orai2, Orai3, Stim1, Stim2 and Saraf which operate as constituents or regulators of CRAC channels and store-operated Ca^{2+} entry (SOCE) in other cell types. Together, our results show that long-term MG stimulation leads to the formation of glycation end products, which facilitates the agonist-evoked Ca^{2+} entry in endothelial cells, and this could be a new pathway that might lead to MG-evoked vasoregression observed in diabetic vasculopathies.

1. Introduction

Chronic hyperglycemia instigates the accumulation of reactive metabolites such as reactive carbonyl (RCS), nitrogen (RNS), and oxygen (ROS) species which evoke(s) post-translational modifications of numerous signalling molecules. In the kidney, reactive metabolites induce cellular imbalance in mesangial cells, endothelial cells and podocytes leading to the development of diabetic nephropathy [1]. Several of these reactive metabolites alter the cellular Ca^{2+} homeostasis in cells susceptible to diabetes late-term complications such as mesangial cells (MC) and endothelial cells (EC).

ROS are formed as a consequence of electron leakage from the mitochondria during the process of oxidative phosphorylation. ROS such as H_2O_2 or O_2^- can oxidize proteins directly or indirectly via the generation of glutathione disulfide (GSSG) from glutathione (GSH) and subsequent modification of cysteine residues by GSSG which is termed

Abbreviations: $[Ca2+]_i$, intracellular calcium; Ang II, angiotensin II; BCNU, bis-chloroethylnitrosourea; CRAC, calcium release activated calcium (channels); EC, endothelial cell; GPCR, G-protein coupled receptors; GSH, glutathione; GSSG, glutathione disulfide; MCEC, mouse cardiac endothelial cells; MG, methylglyoxal; MG-H1, methylglyoxal-hydroimidazolone (adduct); muMEC, murine microvascular endothelial cells; NO, nitric oxide; qPCR, quantitative polymerase chain reaction; RCS, reactive carbonyl species; RNS, reactive nitrogen species; ROCE, receptor-operated calcium entry; ROS, reactive oxygen species; SOCE, store-operated calcium entry; STIM, stromal interaction molecule; TRP, transient receptor potential (channels)

* Corresponding author.
E-mail address: marc.freichel@pharma.uni-heidelberg.de (M. Freichel).

https://doi.org/10.1016/j.ceca.2019.01.002
Received 20 September 2018; Received in revised form 8 January 2019; Accepted 8 January 2019
Available online 09 January 2019
0143-4160/

as S-glutathionylation. Together with nitric oxide (NO), ROS can form the highly reactive RNS peroxynitrite ($ONOO^-$) which can also target cysteine residues in proteins. RCS metabolites such as methylglyoxal (MG) are formed non-enzymatically via de-phosphorylation of dihydroxyacetone phosphate and diacylglycerol during glucose metabolism. Under high substrate (glucose) pressure, such as during diabetes, a several-fold increase in the level of MG is observed which is linked to the development of vasculopathies. As a highly potent glycating agent, MG targets the arginine residues of proteins to form the hydroimidazolone adduct, MG-H1 and other AGEs [2]. MG is considered as highly reactive metabolite contributing to the aggravation of diabetes late-term complications by affecting multiple signalling pathways [3–6], however, its effect on the intracellular Ca^{2+} homeostasis has not been studied in great detail. Signalling events that lead to an increase in intracellular reactive metabolite levels during EC cell dysfunction are initially triggered by peptide mediators such as thrombin, angiotensin II or VEGF-A [7,8]. Downstream activation of Phospholipase C activity leads to an increase in intracellular Ca^{2+} levels which is critically determined by transient receptor potential (TRP) and Orai channels [9–17].

Mammalian transient receptor potential (TRP) channels constitute a superfamily which consists of six subfamilies namely canonical TRPs (TRPC), vanilloid receptor TRPs (TRPV), melastatin TRPs (TRPM), mucolipins TRPs (TRPML), ankyrin TRPs (TRPA1), polycystin TRPs (TRPP). Structurally TRP channels comprise of six transmembrane domains with 5^{th} and 6^{th} transmembrane domain forming the pore of the channel [18].

Orai1, Orai2 and Orai3 proteins form Ca^{2+} conducting channels that are located in the plasma membrane. Orai proteins are activated upon physical interaction with the Ca^{2+} sensor proteins, Stim1 and Stim2, after stimulation of receptors in the plasma membrane and activation of Phospholipase C (PLC) [19]. To this end, Stim proteins present in the membrane of the endoplasmic reticulum (ER) cluster with Orai1 proteins upon depletion of intracellular Ca^{2+} stores. The influx of Ca^{2+} across the plasma membrane is known as receptor-operated Ca^{2+} entry (ROCE) or as store-operated Ca^{2+} entry (SOCE), particularly if the intracellular Ca^{2+} stores were passively depleted by application of inhibitors of the Ca^{2+} ATPases in the ER such as thapsigargin [19,20]. Calcium release activated calcium (CRAC) channels are a prototype of channels mediating SOCE that were initially described in mast cells and lymphocytes [21,22]. The amplitude of SOCE and CRAC currents can be modulated by several small molecule inhibitors such as SKF-96365 [23], Synta66 [24] and GSK-7975 A [25–27] as well as by both overexpression and knockdown/deletion of Orai1, Orai2 and Orai3 proteins [19,25,27–29].

Post-translational modifications of TRP and Orai channels by reactive metabolites accumulating in diabetes may result in alterations in channel opening which can affect the intracellular Ca^{2+} homeostasis and thereby influence various cellular functions. Particularly, cysteine residues of these channels have been subjected to modulation by reactive metabolites and for instance, both S-glutathionylation by GSSG and S-nitrosylation by NO have been reported for TRPC channels [30,31]. The RCS metabolite MG is also capable of increasing intracellular Ca^{2+} in renal tubular cells (MDCK, Madin-Darby canine kidney) and endothelial cells (HUVECs) [32,33]. In another example, acute application of MG to DRG neurons instantaneously increases the Ca^{2+} concentration via TRPA1 channels which is completely abrogated by the application of a TRPA1 blocker (HC-030031) or in *Trpa1*$^{-/-}$ DRG neurons [34]. Similar to the TRP channels, cysteine residues in the Orai and Stim proteins can be modified during oxidative stress and this result in altered activity of these proteins. Particularly, S-glutathionylation of cysteine residues of Stim proteins causes a decrease in Ca^{2+} binding affinity which results in the constitutive Ca^{2+} entry and an increase in basal cytosolic Ca^{2+} levels in lymphocytes [35].

It has been found that chronic (24 h) application of MG increases the intracellular Ca^{2+} concentration in endothelial cells (HUVECs) [33], but the pathways which mediate this Ca^{2+} rise have never been characterized. As the accumulation of MG increases with the progression of diabetes complications [36], therefore it is imperative to study the effect of acute and chronic MG stimulation on the intracellular Ca^{2+} homeostasis in more detail in endothelial cells that are involved in various forms of diabetic vasculopathies.

2. Methods

2.1. Cell lines & primary cells

Two immortalized endothelial cell lines were used for the experiments;

a) SV40 immortalized mouse cardiac endothelial cells (MCECs) were purchased from Biozol/CELLutions Biosystems Inc. (Catalogue No.CLU510). Cells were grown in DMEM media containing 1 g/L glucose supplemented with 5% fetal calf serum, 1% penicillin-streptomycin and 1% HEPES and all growth surfaces were coated with 0.5% gelatin in PBS for 30 min at 37 °C prior to seeding.

b) Functionally immortalized murine endothelial cells (muMECs) that were primarily isolated from lung microvessels (INS-CI-1004) were provided by InSCREENeX GmbH (Braunschweig, Germany) and maintained according to the company's recommendation. muMECs were seeded on 2% gelatin (Sigma-Aldrich, Germany)-coated surface, kept at 37 °C, with 5% CO_2 and appropriate humidity. Experiments with muMECs were done in the passage range of 8 to 13.

c) Primary mouse mesangial cells were purchased from INNOPROT (Derio-Bizkaia, Spain). Cells have been isolated using enzymatic digestion, graded sieving and differential centrifugation as described by Mene et al. [37]. Cells were maintained in the customized mesangial cell media provided along with the cells by INNOPROT.

2.2. Calcium imaging

2.2.1. Seeding of cells and calcium imaging setup

Endothelial cells were cultured until confluency in T75 cm^2 flasks and then seeded on glass coverslips (d = 18 mm) at a density of 1.2×10^4 cells per cm^2. The next day, cells were serum starved for overnight in medium containing 0.1% FCS. Two days after cell seeding, coverslips were transferred to in-house build rectangular chambers, which were then fixed on the stage of an inverted epifluorescence microscope fitted with Fluar 20x objective (Zeiss, Germany) and connected to the continuous perfusion setup (ALA Scientific Instruments, USA). To detect intracellular Ca^{2+}, cells were loaded with the ratiometric calcium indicator, Fura-2 acetoxymethyl ester (2 μM) for 30 min at 37 °C. Cells were alternatively excited at 340 nm and 380 nm with the polychrome V monochromator (Till Photonics, Germany) and emission recordings (510 nm) were obtained after every 5 s using an ORCA Flash 4 camera (Hamamatsu, Japan). The monochromator and camera were controlled by the Axiovision software 4.8.2 (Zeiss, Germany).

2.2.2. Acute stimulation protocol

During acute stimulation protocol, cells were continuously perfused with Ca^{2+} (2 mM) containing physiological standard solution (PSS; 137 mM NaCl, 5 mM KCl, 10 mM HEPES, 10 mM Glucose, 1 mM $MgCl_2$, 2 mM $CaCl_2$) for first 100 s at a temperature of 35 °C using a warming system (Warner Instruments, USA). After 100 s, agonist was applied to the cells in a continuous perfusion mode for the duration of 25 s. After 125 s, cells were again perfused with Ca^{2+} containing physiological solution until the end of the measurement (245 s).

2.2.3. Calcium re-addition protocol

Cells were continuously perfused first, with Ca^{2+} containing PSS for 50 s and then with nominal Ca^{2+} free PSS (EGTA, 150 μM) for another 50 s. Agonists in nominal Ca^{2+} free PSS were applied to the cells at 100 s. At 200 s, Ca^{2+} was re-added along with the agonist until 250 s

and finally, cells were perfused with agonist-free Ca^{2+} containing PSS until the end of the measurements.

2.3. Expression analysis in cell lines using qPCR

To isolate RNA, cells were seeded in T75 cm^2 cell culture flask at a density of 1.2×10^4 cells per cm^2. Next day after the seeding, cells were serum starved in the medium containing 0.1% FCS. Two days after seeding, cells were stimulated with MG (300 μM) for 6 h and subsequently trypsinized, harvested and stored at −80 °C until RNA isolation which was performed with a Qiagen RNeasy mini kit according to the manufacturer's protocol including an on-column cDNA digestion. RNA was isolated from three independent RNA isolations from MCECs and muMECs. cDNA synthesis was carried out using the SensiFAST cDNA synthesis kit (Bioline) according to manufacturer's recommendations. Primers were designed with the online tool provided by Roche (https://lifescience.roche.com/en_de/brands/universal-probe-library.html) and the best primer pair for each target was chosen out of 2–3 from an initial qPCR screen. Quantitative expression analysis was performed using the Universal Probe system (Roche) with the corresponding Fast Start Essential DNA Probes Master (Roche) on a LightCycler 96 Instrument (Roche, Mannheim, Germany). Relative expression levels were obtained by normalising to the expression of the housekeeping genes H3F3A, AIP and CXXC1. Primer sequences can be found in supplement table 1.

2.4. Methylglyoxal stimulation and determination of MG-H1 content

MCECs were seeded into 6-well plates at a density of approx. 5×10^5 cells per well and allowed to adhere for 16 h. Cells were then stimulated with increasing concentrations of MG (0–500 μM) and were harvested (by trypsinization) at various time points (1, 3, 6, 12, 24, 48 h) post-stimulation. Cells were pelleted by centrifugation (1500 rpm; 5 min. at 4 °C) and washed twice with ice-cold PBS. Cells were fixed by resuspension in BioLegend fixation buffer and permeabilized with BioLegend permeabilization buffer, in accordance with the manufacturer's instructions. Cells were then incubated with rat MG-H1 antibody (10 μg/ml in 3% goat serum in PBS; [38]) for 30 min on ice, and washed twice prior to incubation with anti-rat IgG, Alexa Fluor® 488 conjugate (Cell Signaling; 1:1000 dilution in 3% goat serum in PBS) for 30 min on ice. Cells were washed twice with 3% goat serum in PBS and then analysed using a Becton Dickinson LSR II flow cytometer (Heidelberg, Germany) and the FlowJo version xV0.7 (OR, USA).

2.5. Shear stress experiments

Endothelial cells were exposed to laminar shear stress by using a cone-and-plate viscometer as previously described [39]. Upon reaching 100% confluency, 3% vinyl pyrrolidone (V3409, Sigma-Aldrich, Germany) was added to cell culture medium to increase its viscosity, and cells were subjected to unidirectional shear stress (30 dyn per cm^2) for 24 h in a humidified environment with 5% CO_2 at 37 °C. After 24 h, cell culture supernatant and the pelleted cells were separately collected and kept at −80 °C.

2.6. Nitrate assay and western blots

Nitrate in the medium was determined using the Griess Reagent System as an index of the cellular nitric oxide (NO) formation as described previously [40]. For external calibration sodium nitrate (S8170, Sigma-Aldrich, Germany) was diluted in medium covering a concentration range of 0–24 μM nitrate.

Protein detection by Western Blot was done according to standard protocols published previously [41], using the following antibodies against GPx1 (GeneTex, Irvine, CA, USA, GTX116040, 1:1000 dilution), NOS3 (BD Transduction Laboratories, Franklin Lakes, NJ, USA, # 610296, 1:5000 dilution) or β-actin (Abcam, Cambridge, UK, ab6276, 1:5000 dilution).

2.7. Calcium calibration

To calculate the absolute Ca^{2+} concentration in endothelial cells (MCEC and muMEC) and in mesangial cells, cells were first perfused with Ca^{2+} (2 mM) containing PSS for 2 min followed by perfusion with high EGTA (10 mM) containing PSS (zero Ca^{2+}) for 1 min. To obtain minimum fluorescence ratio (R_{min}), cells were kept in high EGTA (10 mM) and ionomycin (10μM) containing PSS for 45 min in a humidified environment with 5% CO_2 at 37 °C and fluorescence ratios were recorded thereafter for 1 min. Subsequently, to obtain maximum fluorescence ratio (R_{max}), cells were treated with high Ca^{2+} (10 mM) containing PSS followed by treatment with ionomycin containing high Ca^{2+} PSS and fluorescence ratios were recorded for approx. 5 min.

Absolute calcium concentration was then calculated with following formula:

$$[Ca2+] = Kd\left(\frac{R - Rmin}{Rmax - R}\right) \times \left(\frac{Fmax,\ \lambda 2}{Fmin,\ \lambda 2}\right)$$

where K_d is dissociation constant for Fura-2 at 37 °C, R is background corrected value of fluorescence ratio, R_{min} is the fluorescence ratio from Ca^{2+} free Fura-2, R_{max} is the fluorescence ratio from Ca^{2+} saturated Fura-2, (F_{max}, λ2/F_{min}, λ2) is denoted as factor β which is F_{max}/F_{min} of Ca^{2+} free form of Fura-2 i.e., 380 nm [42].

2.8. Statistical analysis

Results are shown as mean ± SD unless stated otherwise. For graphics and statistical analysis, Origin (OriginPro 2015, Origin Lab Corporation, USA) was used. Statistical analysis was performed using the appropriate tests depending on the result of the normality tests and test for equal variance.

To test for statistical significance one-way ANOVA was used for Figs. 2, 3A-D and 4, and multiple comparison analysis among different groups was performed using the Tukey test. Two-tailed unpaired student's *t*-test was used for Fig. 3E-G, 5 and 6. Differences with $p < 0.05$ were considered statistically significant. Significances are depicted as * $p < 0.05$, ** $p < 0.01$, and *** $p < 0.001$. For supplementary Fig. 1, Mann-Whitney U test was used to compare two different samples with $p < 0.05$ considered as significantly different. The one sample *t*-test was performed to test for the difference against the control values of the individual no shear stress control taken as 100% (OriginPro 2018 G, Origin Lab Corporation, USA).

3. Results

3.1. Effect of acute MG application on intracellular Ca^{2+} concentration is cell type dependent

A rise in intracellular Ca^{2+} can be evoked following acute application of MG in DRG neurons [34]. We show that such an acute increase in $[Ca^{2+}]_i$ with a time to peak within 30 s can also be seen in primary mesangial cells isolated from mice (Fig. 1A-B), a cell type relevant in the development of diabetic nephropathy [43]. Accordingly, we asked whether similar changes can be observed in endothelial cells by studying MCECs that were acutely challenged with increasing concentrations of MG (100, 500 and 1000 μM) in the presence of extracellular calcium. None of the stated MG concentrations was able to induce any instantaneous changes in the intracellular calcium level in MCECs (Fig. 1C-F). We also tested the effect of acute MG application in muMECs, originally isolated from the lung. These conditionally immortalized ECs retain many characteristic features of native ECs such as shear stress-induced up-regulation of NOS3 and down-regulation of GPx1 expression as well as NO production measured as nitrate in the

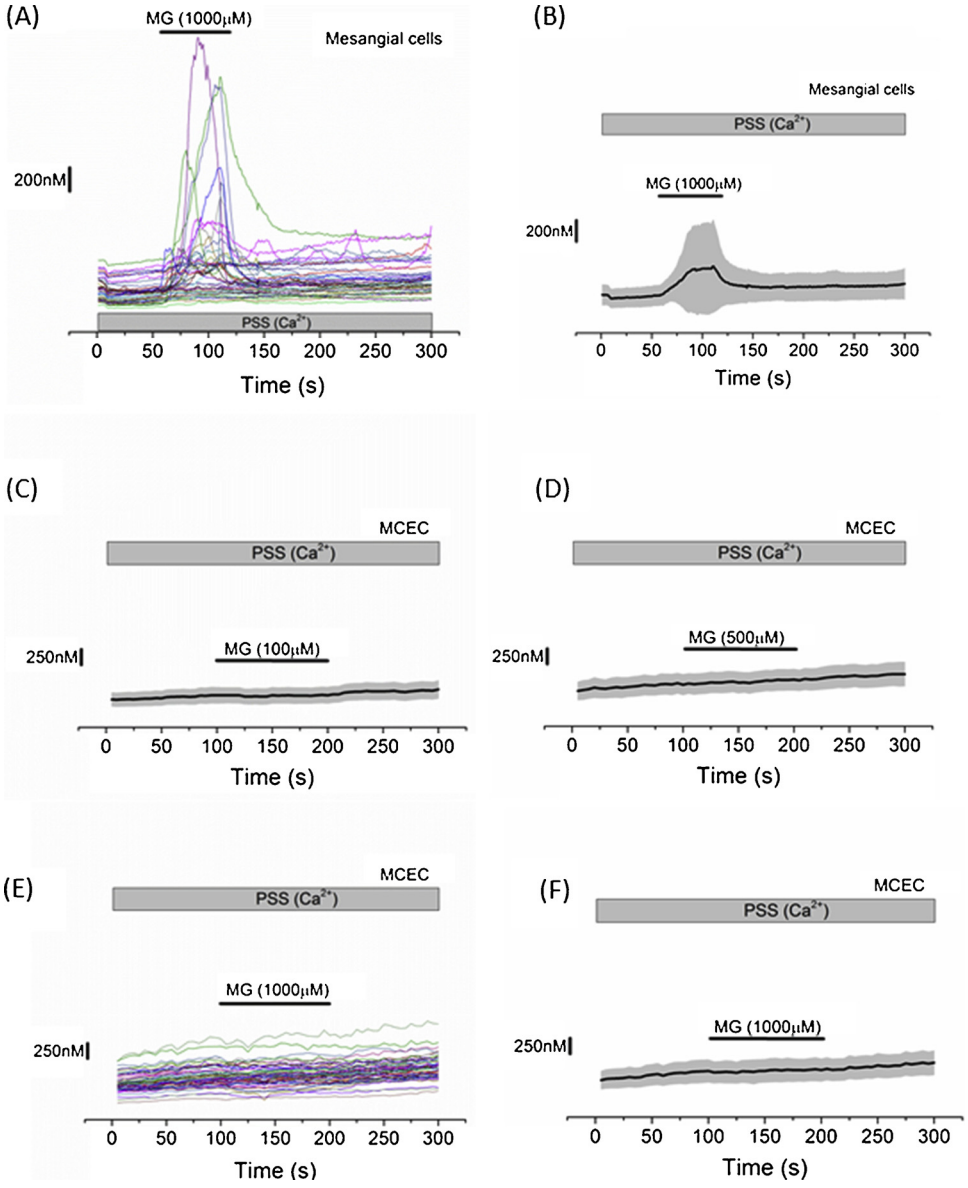

Fig. 1. Effect of acute MG stimulation on intracellular Ca^{2+} levels in mesangial and endothelial cells. (A) Representative single-cell traces of fluorescence ratio (340/380) in primary mouse mesangial cells (n = 3 experiments). MG (1000 μM) was applied for 60 s in the presence of extracellular Ca^{2+}. **(B)** Mean fluorescence ratio from all the cells shown in (A). **(C-D)** Representative mean fluorescence ratio in MCECs (n = 3 experiments). MG concentrations used in C & D were 100 and 500 μM, respectively. MG was applied for 100 s in the presence of extracellular Ca^{2+}. **(E)** Representative single-cell traces of fluorescence ratio in MCECs (n = 3 experiments). 1000 μM MG was applied for 100 s in the presence of extracellular calcium. **(F)** Mean fluorescence ratio of all the cells from (E). For each experiment, more than 50 cells were measured from each coverslip and minimum 3 coverslips were measured in each experiment. The black thick line represents the mean fluorescence ratio and the shaded region represents the SD.

medium/supernatant (Suppl. Fig. 1). Consistent with MCECs, muMECs also lack any acute change in the intracellular Ca^{2+} concentration upon MG application (Supplementary Fig. 2). However, both types of endothelial cells showed a differential instantaneous $[Ca^{2+}]_i$ rise upon application of agonists acting on various GPCRs such as angiotensin II (Ang II), thrombin, ATP, histamine, serotonin and acetylcholine (Supplementary Fig 3 & 4). These results indicate that the MG-induced increase in intracellular Ca^{2+} levels is a cell type-dependent phenomenon and differs particularly between mesangial and endothelial cells.

3.2. MG-induced MG-H1 formation is dependent upon incubation time and concentration

MG is a precursor to advanced glycation end products (AGEs) formation and binding of MG to arginine residues of proteins, leads to the formation of the hydroimidazolone adduct MG-H1. The effect of MG on intracellular Ca^{2+} concentration may therefore not be dependent upon the concentration of MG but the amount of intracellular MG-H1 which is formed at a given concentration. In order to study this effect, a time course of MG-H1 formation in endothelial cells, in response to extracellular MG, was performed. We found that cells incubated with 0, 100 or 200 μM of MG showed no significant increase in the formation of MG-H1 over 48 h (Fig. 2). However, incubation of the cells with 300 and 400 μM MG, respectively, increased the formation of MG-H1 steadily up to 6 h of post-MG incubation. After 6 h, the intracellular MG-H1 content decreased, reflecting the turnover of the MG-H1 modified proteins. At the highest MG concentration (500 μM), MG-H1 content level increased further after 6 h and reaching a peak at 24 h, after which the content decreased rapid, although not returning to baseline, at 48 h. This dramatic difference in MG-H1 content at 500 μM MG may be reflective of a toxic effect in MCECs as seen at this concentration in other cell types [44].

3.3. Methylglyoxal pre-incubation increases agonist-evoked Ca^{2+} entry in MCECs

To establish whether the increased MG-H1 at 6 h was associated with changes in agonist-evoked Ca^{2+} entry, MCECs were pre-incubated with 300 μM MG for 6 h. A calcium re-addition protocol was used to evaluate agonist-evoked Ca^{2+} entry. Like MG, Ang II has been implicated in the development of diabetic vascular pathology [45], and their action might be additive in this direction. Interestingly, Ang II-evoked Ca^{2+} entry was significantly enhanced in MCECs by MG pre-incubation as compared to control conditions (Fig. 3 A, B & D). It is

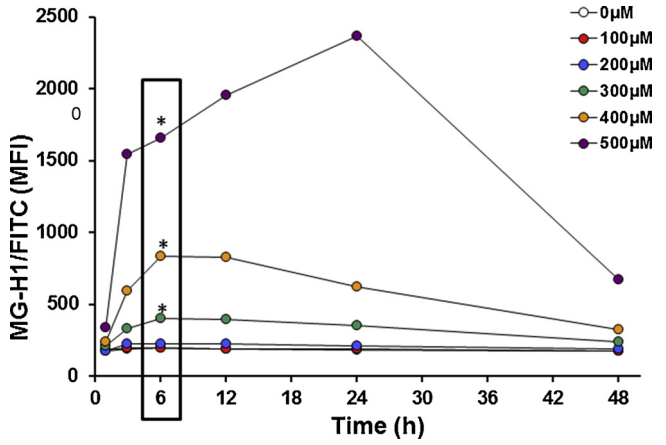

Fig. 2. Time-dependent accumulation of the intracellular MG-H1 content in response to exogenous MG. MCECs were stimulated with increasing concentrations of MG (0–500 μM). Cells were harvested at various time points (1, 3, 6, 12, 24, 48 h) post-stimulation with MG and the MG-H1 content was determined by flow cytometry. Data represent mean ± SD (n = 3 readings for each MG concentration for each time point). Differences in MG-H1 levels after 6 h of MG treatment were compared to the non-treated (0 μM MG) condition. * indicated in the boxed area denotes $p < 0.05$.

known that incubation of cells with MG increases intracellular glutathione disulfide levels, and this can be mimicked experimentally via bis-choloroethylnitrosourea (BCNU) treatment as BCNU inhibits GSSG reductase and subsequently increases GSSG levels [30,46]. Therefore, MCECs were co-stimulated with both MG and BCNU to evaluate potential synergistic effects on Ang II-induced Ca^{2+} entry. However, our results indicate that BCNU application failed to further enhance the effect of MG on Ang II-evoked Ca^{2+} entry (Fig. 3 C &D). Neither pre-incubation with MG alone nor MG plus BCNU evoked a significant change in resting $[Ca^{2+}]_i$ ($F_{340/380}$ 0.66 ± 0.05 for Control, $F_{340/380}$ 0.62 ± 0.06 for MG and $F_{340/380}$ 0.60 ± 0.04 for MG plus BCNU, respectively, n = 4, p = 0.30).

We then tested whether MG pre-incubation also enhances ROCE induced by other GPCR agonists, such as thrombin. The analysis of thrombin-evoked Ca^{2+} entry revealed that pre-incubation with both MG and BCNU significantly boosted the thrombin-evoked Ca^{2+} entry as compared to control conditions (Supplementary Fig. 5A–C). Our results show that MG plus BCNU boosts the Ca^{2+} entry across the plasma membrane whereas Ca^{2+} release from intracellular stores was not significantly affected (46 ± 11% rise in $F_{340/380}$ compared to baseline upon thrombin stimulation in control versus 57 ± 10% $F_{340/380}$ rise in MG plus BCNU, n = 3, p = 0.26).

3.4. MG pre-incubation increases Ang II-evoked Ca^{2+} entry in muMECs

To examine whether the augmentation of ROCE by MG is specific to the MCEC model, we applied these protocols to muMECs. The measurements indicate that the AngII-evoked Ca^{2+} entry was also significantly increased in muMECs after both pre-incubation with MG for 6 h and MG plus BCNU, respectively (Fig. 4A-D). MG pre-incubation in muMECs did not significantly alter AngII-evoked Ca^{2+} release (9.3 ± 4.9% rise in $F_{340/380}$ in Control versus 8.8 ± 2.5% rise in $F_{340/380}$ in MG and 13 ± 5.6% $F_{340/380}$ rise in MG + BCNU, n = 3, p = 0.5).

3.5. ROCE facilitated by MG pre-incubation is abrogated by the CRAC channel inhibitor GSK-7975A

To study which channel entities are involved in the process of increasing Ang-II evoked ROCE by MG pre-incubation, commercially available cation channel blockers were used. First, we were interested in TRPA1 channels which have been shown to be a target of MG in DRG neurons via modification of cysteine residues leading to the increased open probability of TRPA1 channels [34]. Therefore, we tested the role of TRPA1 channels in AngII-mediated ROCE in muMECs by using a similar protocol of 6 h MG pre-incubation and applied the TRPA1 channel blocker HC-030031 (10 μM) 5 min prior to calcium measurements. Compared to the DMSO control, Ca^{2+} entry after Ca^{2+} re-addition was totally unaffected by the TRPA1 blocker (Fig. 5 A–C). Receptor-operated Ca^{2+} entry evoked by AngII induces the depletion of intracellular Ca^{2+} stores via activation of Phospholipase Cβ and generation of IP_3 followed by Ca^{2+} entry through the plasma membrane [47,48]. Therefore GSK-7975 A, that has been shown to block SOCE in many cell types [25] as well as typical CRAC currents [27], was applied to muMECs 5 min prior to calcium measurements. Compared to the

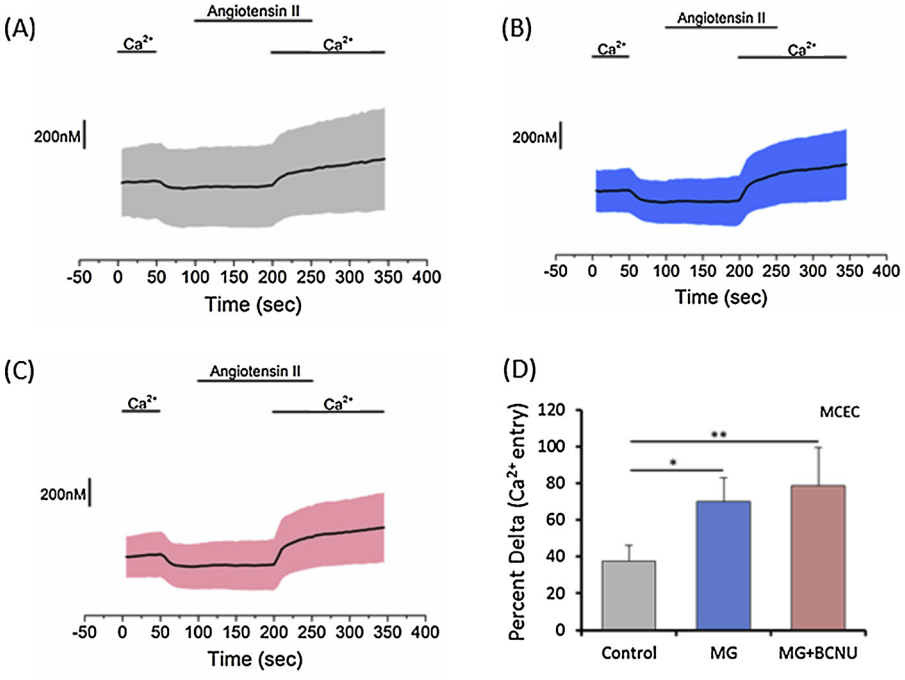

Fig. 3. MG pre-incubation increases Ang II-evoked Ca^{2+} entry in MCECs. A calcium re-addition protocol was used to analyze agonist-evoked Ca^{2+} entry. **(A–C)** Mean fluorescence ratio from 5 independent experiments from (A) control (media), (B) MG (300 μM, 6 h) pre-incubated and (C) MG (300 μM, 6 h) + BCNU (75 μM, 30 min) pre-incubated MCECs. **(D)** Quantification of the relative change of the fluorescence ratio (delta Ang II-evoked Ca^{2+} entry) (n = 5 experiments). Delta was calculated as the percentage difference between the fluorescence ratio before (at 200 s) and after the re-addition of calcium. For baseline fluorescence ratio value, mean of fluorescence ratios from 190 to 200 s was used and compared with the mean of 3 highest peak fluorescence ratio values obtained after Ca^{2+} re-addition. The black thick line represents the mean fluorescence ratio and the shaded region represents the SD. Grey, blue and pink shaded areas represent the Control, MG pre-incubation and MG + BCNU pre-incubation conditions respectively.

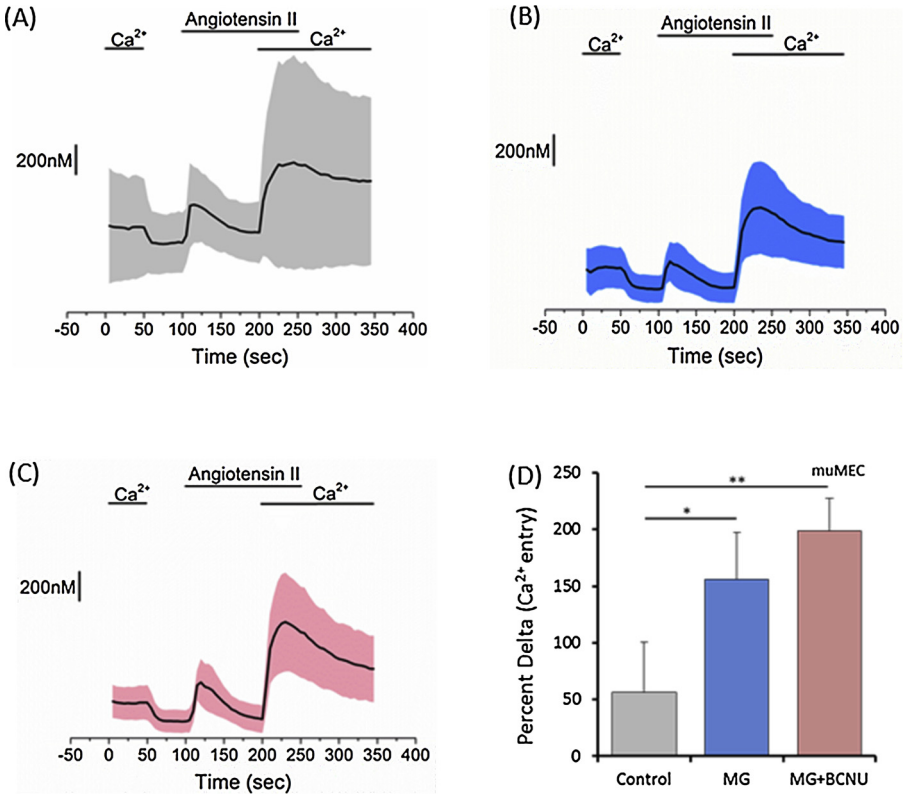

Fig. 4. MG pre-incubation increases the AngII-evoked Ca^{2+} entry in muMECs. (A–C) Mean fluorescence ratio from independent experiments with muMECs from (A) control (n = 4 experiments), (B) MG (300 μM, 6 h) pre-incubated (n = 3 experiments) and (C) MG (300 μM, 6 h) + BCNU (75 μM, 30 min) (n = 3 experiments) pre-incubated muMECs. **(D)** Quantification of the relative change of the fluorescence ratio (delta Ang II-evoked Ca^{2+} entry). Changes in the Ca^{2+} entry were calculated as the percental difference between the fluorescence ratio before (at 200 s) and after the re-addition of calcium. For baseline fluorescence ratio value, mean of fluorescence ratios from 190 to 200 s was used and compared with the average of 3 highest peak fluorescence ratio values obtained after Ca^{2+} re-addition. The black thick line represents the mean fluorescence ratio and the shaded region represents the SD.

DMSO control, pre-incubation with the CRAC channel blocker completely abrogated the AngII-evoked Ca^{2+} entry (Fig. 5 D–F), but not the Ca^{2+} release (17 ± 5% rise in MG-DMSO compared to baseline versus 15 ± 2% in MG + GSK-7975 A, n = 3, p = 0.64). Hence, our results indicate a role of CRAC channels in the AngII-evoked Ca^{2+} entry pathway that is boosted by MG pre-incubation.

3.6. MG pre-incubation does not alter mRNA levels of either AngII and thrombin receptors, TRPA1 or of constituents or regulators of SOCE

To analyse whether the increase in ROCE after MG pre-incubation is due to changes in mRNA expression levels, we performed a qPCR analysis in MCECs and muMECs. Neither the mRNA expression levels of the receptors for angiotensin II (Agtr 1a & Agtr 1b) nor thrombin (PAR1 and PAR4, protease receptors) themselves were changed in MCEC or muMECs (Fig. 6 A & D). TRPA1 mRNA levels (Fig. 6 B & E) were also not altered upon MG pre-incubation. Similarly, mRNA expression levels of constituents of the SOCE pathway (Orai1, Orai2, Orai3, Stim1, Stim2 and Saraf) were not altered (Fig. 6 C & F).

4. Discussion

In this study, we found that the effect of MG on intracellular Ca^{2+} rise differs significantly between mesangial cells and endothelial cells, cell types involved in the development of diabetic long-term complications. While mesangial cells respond with an immediate $[Ca^{2+}]_i$ rise within 30 s after application of MG, we found that only chronic pre-incubation with MG (6 h) augments the ROCE mediated by GPCR agonists such as Angiotensin II in two independent endothelial cell models (MCEC and muMEC). We could show that the MG-mediated increase in AngII-evoked Ca^{2+} entry was abrogated by CRAC channel inhibition with GSK-7975 A, but unaffected by an inhibitor specific to TRPA1 channels, which are known to mediate the acute $[Ca^{2+}]_i$ rise evoked by MG in DRG neurons.

One aspect of the mechanism how MG exerts its effects to aggravate diabetic complications, which has not been studied in much detail, is its influence on the intracellular Ca^{2+} concentration. Calcium overload following MG stimulation consequently activates different signalling pathways [34,36]. Many antioxidants that have been used to prevent MG toxicity were not only shown to decrease endogenous ROS levels but also intracellular Ca^{2+} levels in ECs [33,46]. Endothelial and mesangial cells are highly susceptible to damage by reactive metabolites accumulating during diabetic nephropathy [49,50]. Our results indicate that the acute effect of MG on $[Ca^{2+}]_i$ is strictly cell type-specific as neither of our endothelial cell model showed an instantaneous MG-evoked intracellular Ca^{2+} rise, whereas primary mouse mesangial cells exhibit a rise in $[Ca^{2+}]_i$ within seconds after MG application similar to published observations in primary DRG neurons [34]. Our results substantiate the findings of Jan et al. which showed that the effect of MG on $[Ca^{2+}]_i$ rise is cell type-dependent. In their study, MG induces a significant increase in intracellular Ca^{2+} levels in MDCK cells, it failed to do so in another cell type such as CHOK1, neutrophils or platelets [32].

MG is a precursor of advanced glycated products (AGEs) with the major one being MG-H1 [2,51]. Our results in MCECs showed that formation of MG-H1 was not significantly increased with 100 or 200 μM MG pre-incubation which indicates the efficacy of cellular anti-AGEs defence systems such as cellular proteolysis [52]. However, MCECs incubated with 300 and 400 μM MG, the formation of MG-H1 is induced in a time and concentration-dependent manner with a peak at 6 h. Surprisingly, with 500 μM MG, a fast and strong increase in the MG-H1 levels was seen within a few hours of incubation of MCECs with MG, indicating the toxic effects of MG particularly at this high concentration [44,53].

Increase in the AngII-evoked Ca^{2+} entry by MG pre-incubation was seen in both the endothelial cell lines even though they differ in the source organ, and represent either an immortalized cell line (MCEC) or a functionally immortalized cell type (muMEC). Orai1 and Orai3 have been identified as critical mediators of VEGF-induced ROCE in human umbilical vascular endothelial cells (HUVECs) [47,48]. Furthermore,

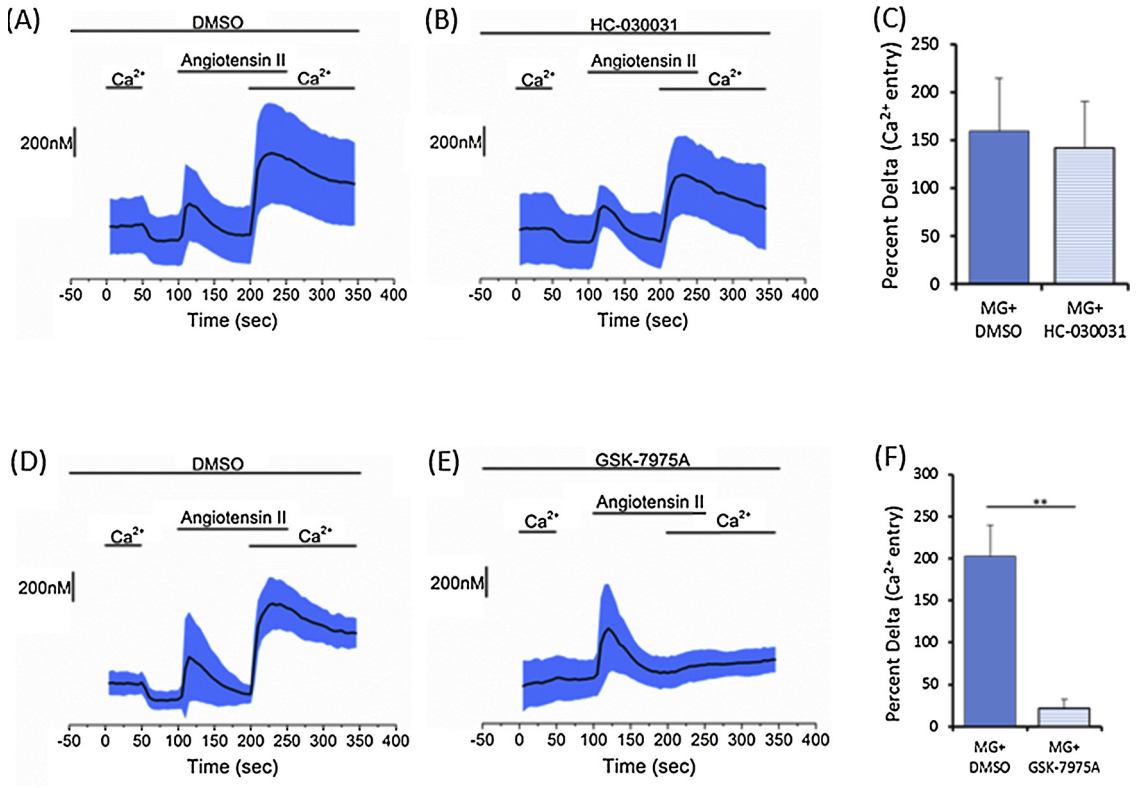

Fig. 5. Increase in Ang II-evoked Ca^{2+} entry by MG pre-incubation is driven by CRAC channels in muMECs. (A-B) Mean fluorescence ratio from 3 independent experiments indicating Ang II-evoked Ca^{2+} entry in (A) DMSO control and (B) TRPA1 inhibitor (HC-030031) (10 μM, 5 min pre-incubation) treated MG pre-incubated muMECs. **(C)** Quantification of Ang II-evoked calcium entry from (A) and (B). **(D & E)** Mean fluorescence ratio from 3 independent experiments indicating Ang II-evoked Ca^{2+} entry in (D) DMSO control and (E) CRAC blocker (GSK-7975 A) (10 μM, 5 min pre-incubation) treated MG pre-incubated muMECs. **(F)** Quantification of Ang II-evoked Ca^{2+} entry from (D) & (E). Changes in the Ca^{2+} entry were calculated as the percental difference between the fluorescence ratio before (at 200 s) and after the re-addition of calcium. For baseline fluorescence ratio value, mean of fluorescence ratios from 190 to 200 s was used and compared with the average of 3 highest peak fluorescence ratio values obtained after Ca^{2+} re-addition. The black thick line represents the mean fluorescence ratio and the shaded region represents the SD.

AngII-evoked Ca^{2+} entry was reduced following Orai1 knock-down in vascular smooth muscle cells [54], but comparable results have not been reported in ECs. Our results emphasize a role of GSK-7975 A-sensitive channels in the AngII-evoked Ca^{2+} entry that is enhanced by MG pre-incubation in our two endothelial cell types. These results suggest that these channels have structural similarities to SOC- or CRAC channels, but our results do not unveil which of these two candidates, i.e. Orai 1 or Orai3, might operate as constituents of the channels that are involved in the MG facilitated ROCE. Further studies are needed to uncover the underlying channel complexes, and qPCR results show that Orai2 is most abundantly expressed in both, MCEC and muMECs, at least on the mRNA level. Analysis of ECs lacking individual Orai proteins or their combinations will be necessary to find out the constituents mediating the observed MG-evoked modulation of ROCE. In another independent study, the influence of MG on Ca^{2+} homeostasis was investigated in adult human retinal pigmented epithelial cells (ARPE), in which application of MG for 6 h increased the basal $[Ca^{2+}]_i$ by 6 fold which was prevented by the application of SOCE blocker, MRS1845. This emphasizes the importance of CRAC channels in mediating an increase in $[Ca^{2+}]_i$ by MG incubation in cells other than ECs [44]. The difference in basal $[Ca^{2+}]$i observed by the above study and in our results could be from the fact that they used an epithelial cell line in contrast to the endothelial cell line we used for our experiments. Several independent studies have characterized TRPA1 channels as being activated by NOX2-produced ROS and this activation facilitates the regulation of EC function such as endothelial-dependent vasodilation [55,56]. Despite being unequivocally identified as targets for MG in DRG neurons [34], TRPA1 channels were not involved in the AngII-evoked Ca^{2+} entry and its modulation by MG in the endothelial cells in our study as tested with TRPA1 blocker HC-030031.

The mechanisms underlying the observed increase in an agonist-evoked Ca^{2+} entry in ECs after MG pre-incubation could be the following: first, MG (and MG plus BCNU) treatment could change the expression of signalling molecules involved in this cascade of receptor-operated Ca^{2+} entry. However, neither the genes encoding the AT1 (Agtr 1a & Agtr 1b) or protease/thrombin receptors (PAR1 & PAR4) were altered on mRNA level, nor the ones for Orai1, Orai2, Orai3, Stim1, Stim2 and Saraf which operate as constituents or regulators of SOCE in other cell types. Second, MG could activate the ion channels by directly modifying them and consequently increasing the ion influx across the membrane. In this regard, MG was shown to activate $Na_v1.8$ channels by binding to arginine residues within their inactivation gate sequence [36]. Furthermore, MG has been identified to activate TRPA1 channels by direct binding to its cysteine residues and subsequent formation of disulfide bonds [34]. In analogy, direct modulation of the constituents forming the GSK-7975 A-sensitive channels in the plasma membrane by MG, possibly Orai proteins could lead to an increase in the open probability of these channels. Moreover, posttranslational modification of Orai and Stim proteins were reported but there is so far no evidence for direct MG-evoked modifications of these proteins. Alternatively, there could be an indirect modulation of these proteins via ROS signalling for instance; MG pre-incubation can increase the intracellular oxidative stress and subsequently boost the production of oxidized glutathione (GSSG) from reduced glutathione (GSH) [57]. GSSG can then potentially modify the cysteine residues via S-glutathionylation which modulates structure and function of the target

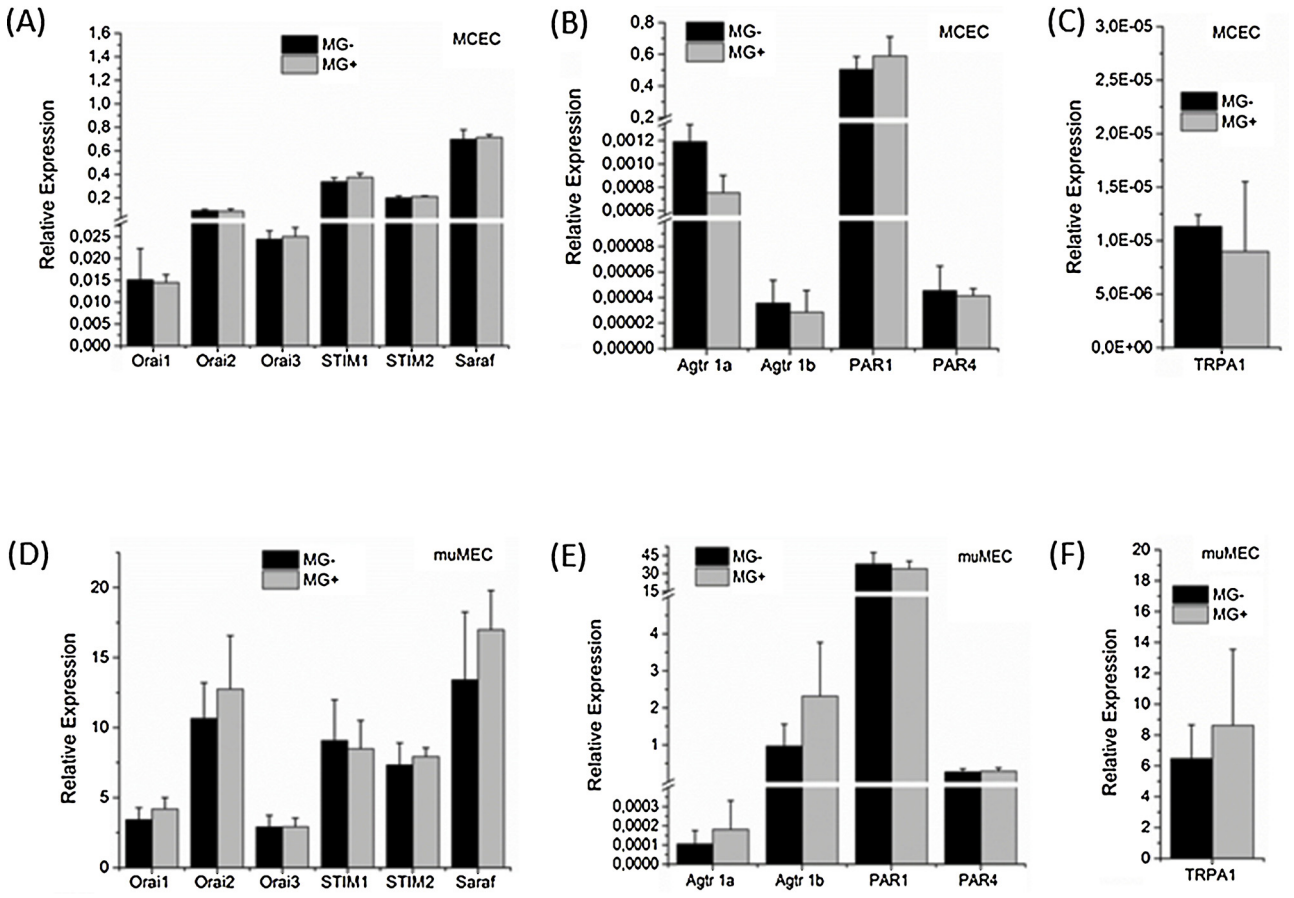

Fig. 6. Quantitative expression analysis of transcripts involved in calcium signalling in endothelial cells. Relative mRNA levels of angiotensin II (Agtr1a & Agtr1b) and protease/thrombin receptors (PAR1 & PAR4), TRPA1, Orai isoforms, Stim1, Stim2 and Saraf, were analysed from independent RNA preparations (n = 3) of (**A-C**) MCECs and (**D-F**) muMECs.

protein. Along these lines, oligomerization and activation of STIM1 proteins by S-glutathionylation during oxidative stress have been shown to increase the SOCE [35,58].

A final consequence of an augmented Ca^{2+}entry by MG pre-incubation is the increase in total $[Ca^{2+}]_i$ concentration and subsequent Ca^{2+} overload might have detrimental effects on the viability of endothelial cells, e.g. by activation of apoptotic processes through multiple pathways [59]. First, exorbitant increase in the $[Ca^{2+}]_i$ induces Ca^{2+} uptake by mitochondria which could promote the opening of mitochondrial permeability transition pore (MPTP) and activate the downstream apoptotic cascade [60,61]. Second, high intracellular Ca^{2+} concentration could activate specific serine proteases termed calpains that are capable of initiating apoptosis by various mechanisms [62,63]. Third, activation of calcineurin phosphatases leads to the de-phosphorylation of various pro-apoptotic proteins, such as members of Bcl-2 family, and thus promotes apoptosis [64]. Lastly, activation of DNA-degrading endonucleases by Ca^{2+} overload has been linked to the initiation of apoptotic processes [65]. Along these lines, pharmacological inhibition or knockdown of Stim1 protects neuronal cell line HT22 from H_2O_2-induced apoptosis by various mechanisms including alleviation of $[Ca^{2+}]_i$ overload, rescuing mitochondrial membrane potential or by reducing the cytochrome c release into the cytosol [66].

Our results indicate that long-term MG pre-incubation leads to an increase in an agonist-evoked Ca^{2+} entry in ECs via CRAC channels in the plasma membrane. These channels are sensitive to the CRAC channel blocker GSK-7975 A suggesting a structural similarity to previously described SOC- or CRAC channels. The initiated Ca^{2+} overload could activate apoptotic signalling in endothelial cells [33] and this might be a mechanism underlying MG-evoked vasoregression described in diabetic vasculopathies. Future studies need to be done to see if an increase in the agonist-evoked Ca^{2+} entry by chronic MG treatment can be corroborated in primary endothelial cells and whether inhibition of Ang II-induced Ca^{2+} entry via CRAC channels can alleviate diabetic vasculopathy.

Funding

This work was supported by the Collaborative Research Centre 1118 (SFB 1118, MF, DS, TF) and the DIAMICOM graduate school, Transregional Collaborative Research Centre 152 (MF), and the DZHK (German Centre for Cardiovascular Research), the BMBF (German Ministry of Education and Research) (MF).

Duality of interest

The authors confirm no duality of interest associated with this manuscript.

Contribution statement

Conceptualization & Design of the study: MF, RS, IM, TF, DS, SH. Methodology: MF, RS, IM, TF, VT, SH, JECL, FM. Investigation & Analysis: RS, SH, TF, AHW, KS, JECL. Writing – Original Draft: RS, MF; Writing – Editing: all authors. Supervision: MF, IM, DS, VT, TF. Funding acquisition: MF, DS.

Acknowledgements

We thank Yoko Oguchi for technical assistance and Juan Eduardo Camacho-Londoño for assistance in statistical analysis of the data.

Appendix A. Supplementary data

Supplementary material related to this article can be found, in the online version, at doi:10.1016/j.ceca.2019.01.002.

References

[1] J.M. Forbes, M.E. Cooper, Mechanisms of diabetic complications, Physiol. Rev. 93 (2013) 137–188.
[2] N. Rabbani, P.J. Thornalley, The critical role of methylglyoxal and glyoxalase 1 in diabetic nephropathy, Diabetes 63 (2014) 50–52.
[3] C. Nigro, G.A. Raciti, A. Leone, T.H. Fleming, M. Longo, I. Prevenzano, F. Fiory, P. Mirra, V. D'Esposito, L. Ulianich, P.P. Nawroth, P. Formisano, F. Beguinot, C. Miele, Methylglyoxal impairs endothelial insulin sensitivity both in vitro and in vivo, Diabetologia 57 (2014) 1485–1494.
[4] A. Riboulet-Chavey, A. Pierron, I. Durand, J. Murdaca, J. Giudicelli, E. Van Obberghen, Methylglyoxal impairs the insulin signaling pathways independently of the formation of intracellular reactive oxygen species, Diabetes 55 (2006) 1289–1299.
[5] T. Chang, R. Wang, D.J. Olson, D.D. Mousseau, A.R. Ross, L. Wu, Modification of Akt1 by methylglyoxal promotes the proliferation of vascular smooth muscle cells, FASEB J. 25 (2011) 1746–1757.
[6] K. Jorgens, S.J. Stoll, J. Pohl, T.H. Fleming, C. Sticht, P.P. Nawroth, H.P. Hammes, J. Kroll, High tissue glucose alters intersomitic blood vessels in zebrafish via methylglyoxal targeting the VEGF receptor signaling cascade, Diabetes 64 (2015) 213–225.
[7] A. Shatanawi, M.J. Romero, J.A. Iddings, S. Chandra, N.S. Umapathy, A.D. Verin, R.B. Caldwell, R.W. Caldwell, Angiotensin II-induced vascular endothelial dysfunction through RhoA/Rho kinase/p38 mitogen-activated protein kinase/arginase pathway, American journal of physiology, Cell Physiol. 300 (2011) C1181–1192.
[8] N.V. Bogatcheva, J.G. Garcia, A.D. Verin, Molecular mechanisms of thrombin-induced endothelial cell permeability, Biochem. Mosc. 67 (2002) 75–84.
[9] K. Klepac, A. Kilic, T. Gnad, L.M. Brown, B. Herrmann, A. Wilderman, A. Balkow, A. Glode, K. Simon, M.E. Lidell, M.J. Betz, S. Enerback, J. Wess, M. Freichel, M. Bluher, G. Konig, E. Kostenis, P.A. Insel, A. Pfeifer, The Gq signalling pathway inhibits brown and beige adipose tissue, Nat. Commun. 7 (2016) 10895.
[10] S. Herroeder, P. Reichardt, A. Sassmann, B. Zimmermann, D. Jaeneke, J. Hoeckner, M.W. Hollmann, K.D. Fischer, S. Vogt, R. Grosse, N. Hogg, M. Gunzer, S. Offermanns, N. Wettschureck, Guanine nucleotide-binding proteins of the G12 family shape immune functions by controlling CD4+ T cell adhesiveness and motility, Immunity 30 (2009) 708–720.
[11] D. Schumacher, B. Strilic, K.K. Sivaraj, N. Wettschureck, S. Offermanns, Platelet-derived nucleotides promote tumor-cell transendothelial migration and metastasis via P2Y2 receptor, Cancer Cell 24 (2013) 130–137.
[12] M. Freichel, S.H. Suh, A. Pfeifer, U. Schweig, C. Trost, P. Weissgerber, M. Biel, S. Philipp, D. Freise, G. Droogmans, F. Hofmann, V. Flockerzi, B. Nilius, Lack of an endothelial store-operated Ca2+ current impairs agonist-dependent vasorelaxation in TRP4-/- mice, Nat. Cell Biol. 3 (2001) 121–127.
[13] P.C. Sundivakkam, M. Freichel, V. Singh, J.P. Yuan, S.M. Vogel, V. Flockerzi, A.B. Malik, C. Tiruppathi, The Ca(2+) sensor stromal interaction molecule 1 (STIM1) is necessary and sufficient for the store-operated Ca(2+) entry function of transient receptor potential canonical (TRPC) 1 and 4 channels in endothelial cells, Mol. Pharmacol. 81 (2012) 510–526.
[14] J.E. Camacho Londono, Q. Tian, K. Hammer, L. Schroder, J. Camacho Londono, J.C. Reil, T. He, M. Oberhofer, S. Mannebach, I. Mathar, S.E. Philipp, W. Tabellion, F. Schweda, A. Dietrich, L. Kaestner, U. Laufs, L. Birnbaumer, V. Flockerzi, M. Freichel, P. Lipp, A background Ca2+ entry pathway mediated by TRPC1/TRPC4 is critical for development of pathological cardiac remodelling, Eur. Heart J. 36 (2015) 2257–2266.
[15] I. Bogeski, R. Kappl, C. Kummerow, R. Gulaboski, M. Hoth, B.A. Niemeyer, Redox regulation of calcium ion channels: chemical and physiological aspects, Cell Calcium 50 (2011) 407–423.
[16] A.P. Arruda, G.S. Hotamisligil, Calcium homeostasis and organelle function in the pathogenesis of obesity and diabetes, Cell Metab. 22 (2015) 381–397.
[17] A. Guerrero-Hernandez, M.L. Gallegos-Gomez, V.H. Sanchez-Vazquez, M.C. Lopez-Mendez, Acidic intracellular Ca(2+) stores and caveolae in Ca(2+) signaling and diabetes, Cell Calcium 56 (2014) 323–331.
[18] S.F. Pedersen, G. Owsianik, B. Nilius, TRP channels: an overview, Cell Calcium 38 (2005) 233–252.
[19] M. Prakriya, R.S. Lewis, Store-operated calcium channels, Physiol. Rev. 95 (2015) 1383–1436.
[20] A.B. Parekh, J.W. Putney Jr., Store-operated calcium channels, Physiol. Rev. 85 (2005) 757–810.
[21] A. Zweifach, R.S. Lewis, Mitogen-regulated Ca2+ current of T lymphocytes is activated by depletion of intracellular Ca2+ stores, Proc. Natl. Acad. Sci. U. S. A. 90 (1993) 6295–6299.
[22] M. Hoth, R. Penner, Depletion of intracellular calcium stores activates a calcium current in mast cells, Nature 355 (1992) 353–356.
[23] S.C. Chung, T.V. McDonald, P. Gardner, Inhibition by SK&F 96365 of Ca2+ current, IL-2 production and activation in T lymphocytes, Br. J. Pharmacol. 113 (1994) 861–868.
[24] A. Di Sabatino, L. Rovedatti, R. Kaur, J.P. Spencer, J.T. Brown, V.D. Morisset, P. Biancheri, N.A. Leakey, J.I. Wilde, L. Scott, G.R. Corazza, K. Lee, N. Sengupta, C.H. Knowles, M.J. Gunthorpe, P.G. McLean, T.T. MacDonald, L. Kruidenier, Targeting gut T cell Ca2+ release-activated Ca2+ channels inhibits T cell cytokine production and T-box transcription factor T-bet in inflammatory bowel disease, J. Immunol. 183 (2009) 3454–3462.
[25] C. Tian, L. Du, Y. Zhou, M. Li, Store-operated CRAC channel inhibitors: opportunities and challenges, Future Med. Chem. 8 (2016) 817–832.
[26] I. Derler, R. Schindl, R. Fritsch, P. Heftberger, M.C. Riedl, M. Begg, D. House, C. Romanin, The action of selective CRAC channel blockers is affected by the Orai pore geometry, Cell Calcium 53 (2013) 139–151.
[27] V. Tsvilovskyy, A. Solis-Lopez, D. Schumacher, R. Medert, A. Roers, U. Kriebs, M. Freichel, Deletion of Orai2 augments endogenous CRAC currents and degranulation in mast cells leading to enhanced anaphylaxis, Cell Calcium 71 (2018) 24–33.
[28] M. Trebak, J.W. Putney Jr., ORAI calcium channels, Physiology 32 (2017) 332–342.
[29] M. Vaeth, J. Yang, M. Yamashita, I. Zee, M. Eckstein, C. Knosp, U. Kaufmann, P. Karoly Jani, R.S. Lacruz, V. Flockerzi, I. Kacskovics, M. Prakriya, S. Feske, ORAI2 modulates store-operated calcium entry and T cell-mediated immunity, Nat. Commun. 8 (2017) 14714.
[30] C. Hong, H. Seo, M. Kwak, J. Jeon, J. Jang, E.M. Jeong, J. Myeong, Y.J. Hwang, K. Ha, M.J. Kang, K.P. Lee, E.C. Yi, I.G. Kim, J.H. Jeon, H. Ryu, I. So, Increased TRPC5 glutathionylation contributes to striatal neuron loss in Huntington's disease, Brain: J. Neurol. 138 (2015) 3030–3047.
[31] T. Yoshida, R. Inoue, T. Morii, N. Takahashi, S. Yamamoto, Y. Hara, M. Tominaga, S. Shimizu, Y. Sato, Y. Mori, Nitric oxide activates TRP channels by cysteine S-nitrosylation, Nat. Chem. Biol. 2 (2006) 596–607.
[32] C.R. Jan, C.H. Chen, S.C. Wang, S.Y. Kuo, Effect of methylglyoxal on intracellular calcium levels and viability in renal tubular cells, Cell. Signal. 17 (2005) 847–855.
[33] P. Chu, G. Han, A. Ahsan, Z. Sun, S. Liu, Z. Zhang, B. Sun, Y. Song, Y. Lin, J. Peng, Z. Tang, Phosphocreatine protects endothelial cells from Methylglyoxal induced oxidative stress and apoptosis via the regulation of PI3K/Akt/eNOS and NF-kappaB pathway, Vascul. Pharmacol. 91 (2017) 26–35.
[34] M.J. Eberhardt, M.R. Filipovic, A. Leffler, J. de la Roche, K. Kistner, M.J. Fischer, T. Fleming, K. Zimmermann, I. Ivanovic-Burmazovic, P.P. Nawroth, A. Bierhaus, P.W. Reeh, S.K. Sauer, Methylglyoxal activates nociceptors through transient receptor potential channel A1 (TRPA1): a possible mechanism of metabolic neuropathies, J. Biol. Chem. 287 (2012) 28291–28306.
[35] B.J. Hawkins, K.M. Irrinki, K. Mallilankaraman, Y.C. Lien, Y. Wang, C.D. Bhanumathy, R. Subbiah, M.F. Ritchie, J. Soboloff, Y. Baba, T. Kurosaki, S.K. Joseph, D.L. Gill, M. Madesh, S-glutathionylation activates STIM1 and alters mitochondrial homeostasis, J. Cell Biol. 190 (2010) 391–405.
[36] A. Bierhaus, T. Fleming, S. Stoyanov, A. Leffler, A. Babes, C. Neacsu, S.K. Sauer, M. Eberhardt, M. Schnolzer, F. Lasitschka, W.L. Neuhuber, T.I. Kichko, I. Konrade, R. Elvert, W. Mier, V. Pirags, I.K. Lukic, M. Morcos, T. Dehmer, N. Rabbani, P.J. Thornalley, D. Edelstein, C. Nau, J. Forbes, P.M. Humpert, M. Schwaninger, D. Ziegler, D.M. Stern, M.E. Cooper, U. Haberkorn, M. Brownlee, P.W. Reeh, P.P. Nawroth, Methylglyoxal modification of Nav1.8 facilitates nociceptive neuron firing and causes hyperalgesia in diabetic neuropathy, Nat. Med. 18 (2012) 926–933.
[37] P. Mene, Mesangial cell cultures, J. Nephrol. 14 (2001) 198–203.
[38] J. Morgenstern, T. Fleming, D. Schumacher, V. Eckstein, M. Freichel, S. Herzig, P. Nawroth, Loss of glyoxalase 1 induces compensatory mechanism to achieve dicarbonyl detoxification in mammalian schwann cells, J. Biol. Chem. 292 (2017) 3224–3238.
[39] M. Cattaruzza, T.J. Guzik, W. Slodowski, A. Pelvan, J. Becker, M. Halle, A.B. Buchwald, K.M. Channon, M. Hecker, Shear stress insensitivity of endothelial nitric oxide synthase expression as a genetic risk factor for coronary heart disease, Circ. Res. 95 (2004) 841–847.
[40] S. Dietrich, J.G. Okun, K. Schmidt, C.S. Falk, A.H. Wagner, S. Karamustafa, A. Radujkovic, U. Hegenbart, A.D. Ho, P. Dreger, T. Luft, High pre-transplant serum nitrate levels predict risk of acute steroid-refractory graft-versus-host disease in the absence of statin therapy, Haematologica 99 (2014) 541–547.
[41] C.S. Sultan, A. Saackel, A. Stank, T. Fleming, M. Fedorova, R. Hoffmann, R.C. Wade, M. Hecker, A.H. Wagner, Impact of carbonylation on glutathione peroxidase-1 activity in human hyperglycemic endothelial cells, Redox Biol. 16 (2018) 113–122.
[42] G. Grynkiewicz, M. Poenie, R.Y. Tsien, A new generation of Ca2+ indicators with greatly improved fluorescence properties, J. Biol. Chem. 260 (1985) 3440–3450.
[43] S. Chaudhari, P. Wu, Y. Wang, Y. Ding, J. Yuan, M. Begg, R. Ma, High glucose and diabetes enhanced store-operated Ca(2+) entry and increased expression of its signaling proteins in mesangial cells, American journal of physiology, Ren. Physiol. 306 (2014) F1069–1080.
[44] C.M. Chan, D.Y. Huang, Y.P. Huang, S.H. Hsu, L.Y. Kang, C.M. Shen, W.W. Lin, Methylglyoxal induces cell death through endoplasmic reticulum stress-associated ROS production and mitochondrial dysfunction, J. Cell. Mol. Med. 20 (2016) 1749–1760.
[45] A.G. Miller, G. Tan, K.J. Binger, R.J. Pickering, M.C. Thomas, R.H. Nagaraj, M.E. Cooper, J.L. Wilkinson-Berka, Candesartan attenuates diabetic retinal vascular pathology by restoring glyoxalase-I function, Diabetes 59 (2010) 3208–3215.
[46] B. Jiang, L. Le, H. Pan, K. Hu, L. Xu, P. Xiao, Dihydromyricetin ameliorates the oxidative stress response induced by methylglyoxal via the AMPK/GLUT4 signaling pathway in PC12 cells, Brain Res. Bull. 109 (2014) 117–126.

[47] J. Li, R.M. Cubbon, L.A. Wilson, M.S. Amer, L. McKeown, B. Hou, Y. Majeed, S. Tumova, V.A. Seymour, H. Taylor, M. Stacey, D. O'Regan, R. Foster, K.E. Porter, M.T. Kearney, D.J. Beech, Orai1 and CRAC channel dependence of VEGF-activated Ca2+ entry and endothelial tube formation, Circ. Res. 108 (2011) 1190–1198.
[48] J. Li, A.F. Bruns, B. Hou, B. Rode, P.J. Webster, M.A. Bailey, H.L. Appleby, N.K. Moss, J.E. Ritchie, N.Y. Yuldasheva, S. Tumova, M. Quinney, L. McKeown, H. Taylor, K.R. Prasad, D. Burke, D. O'Regan, K.E. Porter, R. Foster, M.T. Kearney, D.J. Beech, Orai3 surface accumulation and calcium entry evoked by vascular endothelial growth factor, Arterioscler. Thromb. Vasc. Biol. 35 (2015) 1987–1994.
[49] V.K. Pedchenko, S.V. Chetyrkin, P. Chuang, A.J. Ham, M.A. Saleem, P.W. Mathieson, B.G. Hudson, P.A. Voziyan, Mechanism of perturbation of integrin-mediated cell-matrix interactions by reactive carbonyl compounds and its implication for pathogenesis of diabetic nephropathy, Diabetes 54 (2005) 2952–2960.
[50] A. Pozzi, R. Zent, S. Chetyrkin, C. Borza, N. Bulus, P. Chuang, D. Chen, B. Hudson, P. Voziyan, Modification of collagen IV by glucose or methylglyoxal alters distinct mesangial cell functions, J. Am. Soc. Nephrol. 20 (2009) 2119–2125.
[51] M. Do, S. Kim, S.Y. Seo, E.J. Yeo, S.Y. Kim, Delta-tocopherol prevents methylglyoxal-induced apoptosis by reducing ROS generation and inhibiting apoptotic signaling cascades in human umbilical vein endothelial cells, Food Funct. 6 (2015) 1568–1577.
[52] N. Rabbani, P.J. Thornalley, Advanced glycation end products in the pathogenesis of chronic kidney disease, Kidney Int. 93 (2018) 803–813.
[53] L. Marinucci, S. Balloni, K. Fettucciari, M. Bodo, V.N. Talesa, C. Antognelli, Nicotine induces apoptosis in human osteoblasts via a novel mechanism driven by H2O2 and entailing glyoxalase 1-dependent MG-H1 accumulation leading to TG2-mediated NF-kB desensitization: implication for smokers-related osteoporosis, Free Radic. Biol. Med. 117 (2018) 6–17.
[54] R.W. Guo, L.X. Yang, M.Q. Li, X.H. Pan, B. Liu, Y.L. Deng, Stim1- and Orai1-mediated store-operated calcium entry is critical for angiotensin II-induced vascular smooth muscle cell proliferation, Cardiovasc. Res. 93 (2012) 360–370.
[55] M.N. Sullivan, A.L. Gonzales, P.W. Pires, A. Bruhl, M.D. Leo, W. Li, A. Oulidi, F.A. Boop, Y. Feng, J.H. Jaggar, D.G. Welsh, S. Earley, Localized TRPA1 channel Ca2+ signals stimulated by reactive oxygen species promote cerebral artery dilation, Sci. Signal. 8 (2015) ra2.
[56] S. Earley, A.L. Gonzales, R. Crnich, Endothelium-dependent cerebral artery dilation mediated by TRPA1 and Ca2+-Activated K+ channels, Circ. Res. 104 (2009) 987–994.
[57] P.E. Morgan, P.J. Sheahan, M.J. Davies, Perturbation of human coronary artery endothelial cell redox state and NADPH generation by methylglyoxal, PLoS One 9 (2014) e86564.
[58] R. Bhardwaj, M.A. Hediger, N. Demaurex, Redox modulation of STIM-ORAI signaling, Cell Calcium 60 (2016) 142–152.
[59] A. Kondratskyi, K. Kondratska, R. Skryma, N. Prevarskaya, Ion channels in the regulation of apoptosis, Biochim. Biophys. Acta 1848 (2015) 2532–2546.
[60] C. Giorgi, F. Baldassari, A. Bononi, M. Bonora, E. De Marchi, S. Marchi, S. Missiroli, S. Patergnani, A. Rimessi, J.M. Suski, M.R. Wieckowski, P. Pinton, Mitochondrial Ca (2+) and apoptosis, Cell Calcium 52 (2012) 36–43.
[61] G. Kroemer, L. Galluzzi, C. Brenner, Mitochondrial membrane permeabilization in cell death, Physiol. Rev. 87 (2007) 99–163.
[62] S. Gil-Parrado, A. Fernandez-Montalvan, I. Assfalg-Machleidt, O. Popp, F. Bestvater, A. Holloschi, T.A. Knoch, E.A. Auerswald, K. Welsh, J.C. Reed, H. Fritz, P. Fuentes-Prior, E. Spiess, G.S. Salvesen, W. Machleidt, Ionomycin-activated calpain triggers apoptosis. A probable role for Bcl-2 family members, J. Biol. Chem. 277 (2002) 27217–27226.
[63] M. Chen, H. He, S. Zhan, S. Krajewski, J.C. Reed, R.A. Gottlieb, Bid is cleaved by calpain to an active fragment in vitro and during myocardial ischemia/reperfusion, J. Biol. Chem. 276 (2001) 30724–30728.
[64] H.G. Wang, N. Pathan, I.M. Ethell, S. Krajewski, Y. Yamaguchi, F. Shibasaki, F. McKeon, T. Bobo, T.F. Franke, J.C. Reed, Ca2+-induced apoptosis through calcineurin dephosphorylation of BAD, Science 284 (1999) 339–343.
[65] J.D. Robertson, S. Orrenius, B. Zhivotovsky, Review: nuclear events in apoptosis, J. Struct. Biol. 129 (2000) 346–358.
[66] W. Rao, L. Zhang, N. Su, K. Wang, H. Hui, L. Wang, T. Chen, P. Luo, Y.F. Yang, Z.B. Liu, Z. Fei, Blockade of SOCE protects HT22 cells from hydrogen peroxide-induced apoptosis, Biochem. Biophys. Res. Commun. 441 (2013) 351–356.